FISCHER-TROPSCH SLURRY REACTOR MODELING

Y. Soong, I. K. Gamwo, F. W. Harke,
A. G. Blackwell, and M. F. Zarochak

U.S. Department of Energy
Pittsburgh Energy Technology Center
P.O. Box 10940
Pittsburgh, PA, 15236-0940

For Coal Liquefaction and Gas Conversion Contractors' Review Conference,
Pittsburgh, PA, August 29-31, 1995

FISCHER-TROPSCH SLURRY REACTOR MODELING

Y. Soong, I. K. Gamwo, F. W. Harke, A. G. Blackwell, and M. F. Zarochak

U.S. Department of Energy
Pittsburgh Energy Technology Center
P.O. Box 10940
Pittsburgh, PA 15236-0940

ABSTRACT

This paper reports experimental and theoretical results on hydrodynamic studies. The experiments were conducted in a hot-pressurized Slurry-Bubble Column Reactor (SBCR). It includes experimental results of Drakeol-10 oil/nitrogen/glass beads hydrodynamic study and the development of an ultrasonic technique for measuring solids concentration. A model to describe the flow behavior in reactors was developed.

The hydrodynamic properties in a 10.16-cm diameter bubble column with a perforated-plate gas distributor were studied at pressures ranging from 0.1 to 1.36 MPa, and at temperatures from 20 to 200 °C, using a dual hot-wire probe with nitrogen, glass beads, and Drakeol-10 oil as the gas, solid, and liquid phase, respectively. It was found that the addition of 20 wt% glass beads in the system has a slight effect on the average gas holdup and bubble size.

A well-posed three-dimensional model for bed dynamics was developed from an ill-posed model. The new model has computed solid holdup distributions consistent with experimental observations with no artificial "fountain" as predicted by the earlier model. The model can be applied to a variety of multiphase flows of practical interest.

An ultrasonic technique is being developed to measure solids concentration in a three-phase slurry reactor. Preliminary measurements have been made on slurries consisting of molten paraffin wax, glass beads, and nitrogen bubbles at 189 °C and 0.1 MPa. The data show that both the sound speed and attenuation are well-defined functions of both the solid and gas concentrations in the slurries. The results suggest possibilities to directly measure solids concentration during the operation of an autoclave reactor containing molten wax.

INTRODUCTION

The application of three-phase SBCR systems for coal liquefaction processing is receiving considerable attention. Slurry-bubble-column Fisher-Tropsch (F-T) reactors have many advantages over other types of F-T reactors. Among them are good temperature control of the F-T reaction, the ability to utilize a low H_2/CO ratio synthesis gas, and low mass-transfer resistances.

The important hydrodynamic parameters in the operation of a SBCR are the gas bubble size, holdup, and flow regimes. Hydrodynamic measurements in two-phase systems have been reviewed by several authors (1,2); however, the majority of these studies has been limited to the air-water system. Hydrodynamic measurements using molten wax (typical slurry medium) as the liquid medium are rather limited (3-6). Different hydrodynamic behaviors (e.g., Sauter mean bubble diameter, gas holdup) have been reported in these studies for waxes of similar physical properties. As indicated by Bukur et al.(3), despite similar physical properties among the waxes studied, they showed dissimilar hydrodynamic behaviors. Additional experimental data is clearly required on the hydrodynamic behavior of SBCR

systems using the operating conditions and liquid-phase media of F-T slurry reactors. This information is necessary for a reliable design and scale-up of F-T slurry reactors.

Recently, a three-dimensional hydrodynamic model to describe flow in a bubbling fluidized column with a circular jet was developed. The code was able to predict three-dimensional effects such as a maximum in time-averaged porosities above the jet entrance. However, solid distributions in the free board consistently displayed a "fountain" artifact that was not observed experimentally. It was found that the equation system possesses potential complex-valued characteristics and hence is ill-posed as an initial-value problem (7,8). The above model is modified to a well-posed model referred to as model B (9). The new three-dimensional model has predicted solid holdup distributions with no artificial "fountain." This is consistent with the experimental observations.

To design and efficiently operate a SBCR, the degree of dispersion of the solid (catalyst) in the SBCR must be understood and controlled. The catalyst concentration along the column greatly affects the operation of the SBCR. Measurements must be made under reaction conditions to fully understand the influence of various reaction, reactor, and catalyst parameters on the catalyst concentration profile in the reactor and the effect of catalyst distribution on the overall conversion and product selectivity. A recent method involving the measurement of ultrasound transmission in a slurry-phase stirred-tank reactor offers the possibility of using the ultrasonic technique for the measurement of solids concentration in a SBCR (10). When the velocity of sound in a liquid (1324 m/sec at 25°C for kerosene) is significantly different from that in a solid (5968 m/sec at 25°C for fused silica), a time shift and an amplitude change in the sound wave relative to those for the pure liquid can be detected when solid particles are present. The solids concentration in a slurry reactor can be determined by measuring the amplitude and time shift of an ultrasonic pulse in the slurry medium. The development of this ultrasonic technique will permit the measurement of catalyst concentration during reaction in a SBCR.

The objectives of this project are to study the hydrodynamics in a hot-pressurized SBCR, develop experimentally verified hydrodynamic models, and a diagnostic technique for the direct measurement of slurry concentrations in SBCR. The ultimate goal is to develop a data base which would provide reliable estimates of hydrodynamic parameters relevant to design and operation of the Fischer-Tropsch (F-T) slurry reactors.

EXPERIMENTAL FACILITIES

A schematic diagram of our SBCR is reported elsewhere (11). The unit consists of two stainless steel columns, each of which has an internal diameter of 10.16 cm and a height of 244 cm. The column in which the hydrodynamic studies were conducted has 12 different axial locations for data collection. Experiments were conducted in batch-mode operation (continuous flow of gas and a stationary liquid). The local gas holdup, bubble diameter, bubble velocity, and bubble size distribution were measured by inserting a dual hot-wire probe horizontally into the column at any of the 12 positions and moving it to the desired radial position. The details of the dual hot-wire probe and an integrated data acquisition and analysis system have been described elsewhere (11). The experiments were conducted at temperatures ranging from 20 to 200 °C, at pressures from 0.1 to 1.36 MPa, and at superficial gas velocities of up to 9 cm/sec with the Drakeol-10 oil as the liquid-phase medium, nitrogen as the gas-phase medium, and 20 wt% of glass beads (80 ± 5 microns in diameter) as the solid-phase medium.

The detail of the 2.5-liter autoclave reactor used for the ultrasonic investigation was reported elsewhere (11). Nitrogen bubbles were introduced through a sintered frit at the bottom of

the reactor. The nitrogen flow was controlled electronically to a maximum of 400 mL/min by a mass-flow controller. Glass beads (80 ± 5 microns in diameter) were used as the solid in the slurry. The solids concentration (solid weight/liquid weight) was varied from 1 to 25 wt% for each nitrogen flow in the reactor. Molten paraffin wax (Fischer Scientific, P-22) at a temperature of 189 °C was used as the liquid medium. Experiments were conducted at 0.1 MPa. Ultrasonic pulses were generated using lithium niobate transducers at a frequency of 2.5 MHz. The transducer and receiver were mounted directly inside a metal delay line which was screwed into a fitting inside the reactor wall. Ultrasonic measurements were made by using a computer-based TestPro system manufactured by Infometrics Inc.

RESULTS AND DISCUSSIONS

HYDRODYNAMIC STUDY

Figure 1 shows the effect of gas superficial velocity on axial gas holdups on the nitrogen/Drakeol-10 oil/glass beads (20 wt%) system in the bubble column at ambient conditions. At gas velocity up to 4.36 cm/sec, the axial gas holdup profiles in the column were rather uniform; however, at gas velocity of 5.26 cm/sec, there was a noticeable change in the gas holdup at height of 150 cm above the gas distributor. At a higher gas velocity of 7.05 cm/sec, axial gas holdup increases significantly in the column. It increased from 0.06 at the bottom of the column to 0.72 at the top of the column.

Figure 2 illustrates the Sauter mean bubble diameters versus the superficial gas velocity on the nitrogen/Drakeol-10 oil/glass beads (20 wt%) system in the bubble column at ambient conditions. As shown in Figure 2, the Sauter mean bubble diameters were approximately 2 cm for most superficial gas velocities. The Sauter mean bubble diameters were affected by the distance above the gas distributor, when the superficial gas velocity changed from 5.26 to 7.05 cm/sec. A significant change on the Sauter mean bubble diameter was observed along the axial direction of the column, it increased from 2 cm at the bottom to 9.6 cm at the top of the column. The presence of solids in the bubble column reactors further complicates the flow pattern. As reported by Matsura and Fan (12), similar to two-phase bubble columns, three main flow regimes can be distinguished in the system, namely the homogeneous, heterogeneous, and slug flow regimes. Results from Figures 1 and 2 can be combined to describe the flow regimes. At low gas velocities, smaller than 4 cm/sec, the homogeneous bubble regime exists. The transition from homogeneous bubbling to slug regime may occur for gas velocities ranging from 4 to 6 cm/sec. The slug flow occurred for gas velocity above 6 cm/sec.

Figure 3 shows the effect of 20 wt% glass beads on the Sauter mean bubble diameter in nitrogen/Drakeol-10 oil system in the bubble column at ambient conditions. The results were obtained at the same conditions except that one was collected in a two-phase system and the other in a three-phase system. The Sauter mean diameter decreased slightly after the addition of 20 wt% of glass beads in the system.

Figure 4 illustrates the effect of 20 wt% glass beads on the Sauter mean bubble diameter on the nitrogen/Drakeol-10 oil system in the bubble column at 200 °C and 1.36 MPa. The results were again obtained at the same conditions except one was collected in a two-phase system and the other in a three-phase system. The Sauter mean diameter collected from the two-phase system was approximately the same as that obtained from the three-phase system. However, at higher gas velocities, 6 cm/sec or higher, the Sauter mean diameter obtained from the three-phase system was higher than that collected from the two-phase system. The Sauter mean bubble diameter profiles in the bubble column were rather uniform at both conditions. Thus, one can infer that the superficial gas velocity did not have any

effect on the Sauter mean bubble diameter at the above conditions.
Figure 5 shows the effect of 20 wt% glass beads on the average gas holdup for experiments conducted at ambient conditions. The average gas holdup was found to increase linearly with increasing superficial gas velocity. It can be seen from the data that the addition of 20 wt% glass beads in the system has only a slight effect on the observed average gas holdup. Our results are consistent with the results reported in the literature, i.e., the presence of solid generally decreases the gas holdup. Joosten et al. (13) observed that the gas holdup values at high solids concentrations (>15%) are lower and gas bubbles are larger, so bubble coalescence apparently takes place at a higher frequency. Several authors (14-16) concluded that an increase in solids concentration generally decreases the gas holdup, but the effect becomes insignificant at high gas velocity (>0.1 m/sec). Chabot and de Lasa (17) conducted the three-phase studies using a zinc-copper oxide catalyst (dp = 12.5 μm) suspended in a paraffin oil. They concluded that, in general, the presence of small solid particles reduces the gas holdup, due to an increase in the slurry viscosity. The influence of the solid is higher at lower superficial gas velocities, decreasing gradually with increasing gas velocity, and becomes imperceptible at the highest gas velocity studied (14.7 cm/sec). Due to the scare of data at higher gas velocities, we were not able to confirm our results with those in the literature.
Figure 6 illustrates the effect of 20 wt% glass beads on the average gas holdup in nitrogen/Drakeol-10 oil system in the bubble column at 200 °C and 1.36 MPa. Again, the results were obtained at the same conditions except one was collected in a two-phase system and the other in a three-phase system. The average gas holdup collected from the two-phase system was approximately the same as that obtained from the three-phase system. However, under the higher gas velocities conditions, 6 cm/sec or higher, the average gas holdup obtained from the three-phase system was higher than that collected from the two-phase system. Inconsistencies in the solids effect on gas holdup were also reported in the literature. Kuo (4) reported that when a very low (2 wt%) catalyst loading was used with Mobil reactor wax, the gas holdup at 260 °C and 0-6 cm/sec superficial gas velocity was about 9% lower than that obtained without any catalyst. A different picture was described by Bukur et al. (18) based on the experiments with iron-oxide particle suspended in FT-300 wax. The addition of 0-5 μm solid particles increased gas holdup and the 20 wt% concentration had the maximum effect in the small column. The addition of particles (20-44 μm) in the large column (0.21 m) increased the gas holdup at ug < 0.04 m/sec and had no effect at ug > 0.08 m/s.

MATHEMATICAL MODEL

The well-posed model, i.e., one possessing all real characteristics was first given by Rudinger and Chang (19) who analyzed non-steady one-dimensional two-phase flow. Saltanov (20) solved such a problem for steady two-dimensional supersonic flow over an airfoil. Lyczkowski (21) generalized the Rudinger-Chang equations.
The fundamental differences between the ill- and well-posed models appear in the phases momentum and the drag coefficient. In the well-posed model, all pressure drops are in the gas-phase momentum equations. The drag coefficient is modified to satisfy Archimedes' principles (9) and the usual minimum fluidization relationship as given by Kunii and Levenspiel (22). The differential equations and constitutive relations are written below. In the following equations, R=1 for the rectangular coordinates; R=r for the symmetric cylindrical coordinates, where r is the radial coordinate.

Continuity equation for phase k (= g, s)

$$\frac{\partial}{\partial t}(\epsilon_k \rho_k) + \frac{1}{R}\nabla\cdot(R\,\epsilon_k \rho_k \vec{v}_k) = 0 \qquad (1)$$

$$\sum_k \epsilon_k = 1.0 \qquad (2)$$

Gas-phase momentum equation k = (g; l ≠ g)

$$\frac{\partial}{\partial t}(\epsilon_g \rho_g \vec{v}_g) + \frac{1}{R}\nabla\cdot(R\,\epsilon_g \rho_g \vec{v}_g \vec{v}_g) =$$

$$-\nabla p_g + \epsilon_g \rho_g \vec{g} + \frac{1}{R}\nabla\cdot(R\bar{\bar{\tau}}_g) - \tau_{g0}\frac{1}{R}\nabla R \qquad (3)$$

$$+ \sum_{l=1}^{N} \beta_{gl}(\vec{v}_l - \vec{v}_g)$$

Gas-phase stress

$$\bar{\bar{\tau}}_g = \epsilon_g \mu_g[\nabla\vec{v}_g + (\nabla\vec{v}_g)^T] - \frac{2}{3}\epsilon_g \mu_g \frac{1}{R}\nabla\cdot(R\vec{v}_g)\bar{\bar{I}} \qquad (4)$$

$$\tau_{g0} = 2\epsilon_g \mu_g \frac{1}{R}\vec{v}_g\cdot\nabla R - \frac{2}{3}\epsilon_g \mu_g \frac{1}{R}\nabla\cdot(R\vec{v}_g) \qquad (5)$$

Solids-phase momentum equation k (=s; l≠s)

$$\frac{\partial}{\partial t}(\epsilon_s \rho_s \vec{v}_s) + \frac{1}{R}\nabla\cdot(R\epsilon_s \rho_s \vec{v}_s \vec{v}_s) =$$

$$\epsilon_s \rho_s \vec{g} + \frac{1}{R}\nabla\cdot(R\bar{\bar{\tau}}_s) - \tau_{s0}\frac{1}{R}\nabla R - \sum_{l=1}^{N} \beta_{sl}(\vec{v}_l - \vec{v}_g) \qquad (6)$$

Solids-phase stress

$$\bar{\bar{\tau}}_s = -p_s\bar{\bar{I}} + 2\epsilon_s \mu_s \bar{\bar{S}}_s \qquad (7)$$

$$\tau_{s0} = -p_s + 2\epsilon_s \mu_s[\vec{v}_s\cdot\frac{1}{R}\nabla R - \frac{1}{3R}\nabla\cdot(R\vec{v}_s)] \qquad (8)$$

Deformation rate

$$\bar{\bar{S}}_s = \frac{1}{2}[\nabla\vec{v}_s + (\nabla\vec{v}_s)^T] - \frac{1}{3R}\nabla\cdot(R\vec{v}_s)\bar{\bar{I}} \qquad (9)$$

Solid-phase pressure

$$p_s = p_s(\epsilon_s) \qquad (10)$$

and

$$\nabla p_s = G(\epsilon_s)\nabla \epsilon_s \tag{11}$$

with

$$G(\epsilon_s) = 10^{(8.76\epsilon_s - 1.33)} \ dynes/cm^2 \tag{12}$$

Gas-solid drag coefficients

for $\epsilon_g \leq 0.8$, (*based on Ergun equation*)

$$\beta = 150\frac{\epsilon_s^2 \mu_g}{\epsilon_g^2 d_p^2} + 1.75\frac{\rho_g \epsilon_s |\vec{v}_g - \vec{v}_s|}{\epsilon_g d_p} \tag{13}$$

for $\epsilon_g > 0.8$, (*based on empirical correlation*)

$$\beta = \frac{3}{4} C_d \frac{\epsilon_g \epsilon_s \rho_g |\vec{v}_g - \vec{v}_s|}{d_p} \epsilon_g^{-1.65} \tag{14}$$

$$C_d = \begin{cases} \dfrac{24}{Re_p}[1 + 0.15 Re_p^{0.687}], & for\ Re_p \leq 1{,}000 \\ 0.44 & for\ Re_p > 1{,}000 \end{cases} \tag{15}$$

where

$$Re_P = \frac{\epsilon_g \rho_g |\vec{v}_g - \vec{v}_s| d_p}{\mu_g} \tag{16}$$

Equation of state

$$\rho_g = \frac{p_g}{RT} \tag{17}$$

$$\rho_k = \rho_s \quad for\ k \neq g. \tag{18}$$

The well-posed hydrodynamic code was used to simulate the flow in a fluidized column with a circular jet. The column cross sections were 40 cm by 3.81 cm. The jet nozzles were

1.27 cm O.D copper tubing. Air is supplied by three separate streams: two for the air plenum supplying air to fluidize the bed particles, and one for the air jet. The computation was done in one quarter of the bed due to the assumption of symmetry in both the X and Y directions. The solid material was Ottawa Sand with actual density of 2610 kg/m^3, a settled bulk density of 1562 kg/m^3, and a mean particle diameter of 503 μm. The minimum fluidization velocity was 25.9 cm/s and the packed-bed voidage was 0.45. The nonuniform finite difference grids used in the computation are shown in Figure 7. Numerical error that arises in the solution of the Navier-Stokes equations when a nonuniform mesh is used was minimized by proper assignment of cell sizes $(\Delta_{i+1}/\Delta_i) \leq 1.25$ which provided maximum accuracy and minimum computation time. The total number of grids was 14x38x8 (4256 nodes). The time step Δt was 10^{-5} second during the first second of the simulation and 4 x 10^{-5} up to 2 seconds. The computer code was run on a CRAY supercomputer.

The solid holdup distributions predicted by the ill-posed model (previous version (23)) and the well-posed model (present version) are compared with a sketch of the experiment results in Figure 8. It clearly shows that the well-posed model predictions are consistent with the sketch of the experiment. Thus, we have cured the ill-posedness of the initial value problem as evidenced by the disappearance of the artificial fountain.

ULTRASONIC INVESTIGATION

Figure 9 shows the change in the amplitude ratio of the transmitted ultrasonic signals A/A_o in the reactor as a function of nitrogen flow at 189 °C. A and A_o are the amplitudes of the transmitted signals with and without the presence of nitrogen, respectively. Figure 9 also indicates that the amplitude ratio is approximately an inverse exponential function of the nitrogen flow. When a sound wave strikes the boundary between two different media and the acoustic impedances of the two media are different, part of the acoustic energy will be reflected and some will be transmitted. Acoustically, the impedance's of two media will determine the transmission of the wave from one medium to another and the amount of reflection of sound at the boundary between two media. If the impedances of two media are widely separated, e.g. nitrogen and paraffin wax, then most of the energy is being reflected back in the first medium (paraffin wax) with little transmission into the second medium (nitrogen). It can be assumed that the ultrasonic pulse cannot penetrate through much of the nitrogen-paraffin wax interface in the current experimental frequency due to the acoustic impedance mismatch of this combination. Since the ultrasound beam cannot penetrate nitrogen bubbles that lie in its path, the amount of attenuation of the ultrasound beam by nitrogen bubbles is proportional to the amount of gas in the form of bubbles present in the path. We also estimated the bubble sizes to be around 2 mm in the path between the transducer and the receiver within the range of flow studied. The decreasing of A/A_o as the nitrogen flow increased appears related to the nitrogen bubbles. Chang et al. (24) measured void fractions up to 20% in bubbly air-water two-phase flow using an ultrasonic transmission technique. Their results showed that the transmitted ultrasonic signal could be approximated by the exponential relationship :

$$A/A_o = \exp [-f(d_b)\, \epsilon] \qquad (19)$$

where ϵ is the void fraction and $f(d_b)$ is a function dependent on the Sauter mean diameter. This correlation shows that the A/Ao ratio has exponential relationship with both the void fraction and a function dependent on the bubble diameter. The effect of air bubble diameter on A/Ao ratio was found to be significant where A/Ao decreased with increasing bubble size. Bensler et al. (25) also conducted the measurement of interfacial area in bubbly flows in air-water systems by means of an ultrasonic technique. Their observations showed that the

transmitted ultrasonic signal could also be expressed by the exponential-relationship :

$$A/A_o = \exp [\Gamma x/8\ S(kd_b/2)] \qquad (20)$$

where Γ is the volumetric interfacial area, x is the travel distance in the path, S is the scattering coefficient, k is the wave number of the ultrasonic wave which surrounds the bubble, and d_b is the Sauter mean bubble diameter. Equation (20) shows that the A/Ao ratio has exponential relationship with the interfacial area and the scattering cross section which is a function dependent on both the bubble radius and the wave number of the ultrasonic wave surrounding the bubble. Our observations of A/Ao in the nitrogen/paraffin wax system are in qualitative agreement with those reported by Chang et al. (24) and Bensler et al. (25). The decreasing A/Ao ratio as the nitrogen flow increased in Figure 9, may be attributed to the combination of the void fraction, bubble size and the scattering cross section. Figure 9 also illustrates the effect of the nitrogen flow on the transit time, t_b. It was approximately 140.25 μsec at all nitrogen flows. It is evident that the transit time was unaffected by the nitrogen flow within the current experimental conditions. The results indicate that only the amplitude and not the transit time of the ultrasonic signal are affected by the nitrogen flow rate in the reactor within the current experimental conditions. Chang et al. (24) also reported that the amplitude of the transmitted sound pulses depends significantly on the number of bubbles; however, the transit time does not change with the void fraction. Our results obtained from the nitrogen/molten wax system are similar to those of Chang et al. (24) for the air/water system.

The solids concentration in a three-phase slurry has a significant effect on both amplitude ratio and transit time, t_b, of an ultrasonic signal. Figure 10 shows the effect of solids concentration on the amplitude ratio of the transmitted ultrasonic signal A/A_o (A and A_o are the transmitted signals with and without the presence of solids, respectively) in the autoclave at a constant temperature of 189 °C and with a constant stirring speed and without nitrogen flow. A/A_o decreases with increasing solids concentrations. Figure 10 also presents the effect of the solids concentration on the transit time, t_b. It was approximately 140.25 μsec with no solids; however, it decreased to approximately 139.25 μsec as the solids concentration increased to 25 wt%. In general, the amplitude of the transmitted ultrasonic signals and transit time decreased as the solids concentration increased. When an ultrasonic pulse is sent across the slurry reactor, the amplitude of the pulse is reduced when it strikes a solid in the slurry because the pulse is partially scattered and absorbed. Scattering is often the predominant form of attenuation in heterogenous materials. It occurs when some of the ultrasonic wave incident upon a discontinuity in a material, for example, solid particle, is scattered in directions which are different from that of the incident wave. The unscattered pulse is transmitted through the solid to the receiver. The amplitude of the transmitted portion of the pulse is measured by the receiver located on the opposite side of the autoclave. The more particles present in the path, the less transmitted pulse will be detected. The amplitude ratio of the pulse is inversely proportional to the quantity of solid particles present in the path. Therefore, the measured amplitude of the sound wave transmitted through a slurry mixture is expected to be a strong function of the concentration of solids. The transit time decreased as the solids concentration increased in the reactor. Since sound waves travel at a much faster velocity in the solid (5571 m/sec for fused silica at 189 °C) than in the paraffin wax (943 m/sec at 189 °C), the transit time of the transmitted ultrasonic pulse should depend on the quantity of solid particles present in the path. The higher the concentration of solid particles are present in the path, the shorter the transit time would be observed.

Figure 11 shows the effect of solids concentration on the transit time as a function of

nitrogen flow. The solids concentration has a significant effect on the transit time at a constant flow of nitrogen of 100 mL/min: it was approximately 140.20 μsec at 2 wt%, decreased to approximately 139.79 μsec as the solids concentration increased to 15 wt%, and decreased further to approximately 139.27 μsec as the solids concentration increased to 25 wt%. As discussed earlier, sound waves travel at a much faster velocity in the solid than in the paraffin wax, the transit time of the transmitted ultrasonic pulse should depend on the quantity of solid particles present in the path. The higher the concentration of solid particles present in the path, the less the transit time would be observed. We speculate that the decrease of transient time as the solids concentration increased is due to the number of solid particles present in the path. It was interesting to note that the presence of nitrogen bubbles affect the transit time. For most cases, the presence of more nitrogen bubbles causes a slightly decreased in transient time. It should be noted that the principal effect of the nitrogen bubbles is to improve the suspension of the beads, thereby increasing the attenuation and decreasing the transit time over the values obtained with the stirrer alone. Separate tests with the stirrer and nitrogen bubbles in the absence of beads confirm that their presence alone causes no effects on the transit time (Figure 9). Figure 11 further illustrates the fractional change in transit time $\Delta t/t_o$ ($\Delta t = t_a - t_b$) as a function of solids concentration under different nitrogen flows. The fractional change in transit time (time ratio) increased as the solids concentration increased. The results illustrated in Figure 11 can be described by a simple model in which it is assumed that the presence of solid particles in the path of the sound wave reduces the transit time because the sound velocity in the solid is faster than that in the liquid. If the solid particles are assumed to be randomly distributed, the time ratio $\Delta t/t_o$ is related to the concentration fraction ω by the equation.

$$\Delta t/t_o = \alpha\, \omega^{1/3}(1 - v_l/v_s) \qquad (21)$$

Here α is a constant for particles of a given composition and v_l and v_s are the speed of sound in the liquid and solid, respectively. A derivation of this equation is given elsewhere (26). The above equation, which predicts that the time ratio should be dependent upon solids concentration, is approximately the case in experiments presented here for solids well-suspended in the liquid phase. However, it is clear that the functionality of the predicted dependence on solids concentration does not adequately describe the data. The observed dependence is closer to a linear rather than a cube root dependence on ω. This discrepancy is perhaps not surprising because equation (21) is only expected to be true for $\omega << 1$, and this condition is violated over the range of solids concentration investigated here. It should be noted that the simple model (assuming that the ultrasound wave can transmit through the nitrogen bubble) predicts that the number of nitrogen bubbles in the liquid should increase the transit time, because the speed of sound in nitrogen is less than that in the liquid. This increase will not be observed in the current experimental set-up due to the acoustic impedance mismatch, and will not affect our measurements. The signal that we measured was not transported through the nitrogen and therefore showed no change in transit time with increasing nitrogen flow.

In concentrated systems, multiple scattering is important, i.e. a significant proportion of the energy scattered from one particle is incident upon neighboring particles (27). The velocity of the sound and attenuation depends on particle size as well as concentration under this condition (28). Two important parameters - the ultrasound wave number, k, and the radius of the particle, a - are often utilized to describe the ultrasound propagation and attenuation. For this study, the ka range is around 1.3. As indicated previously, the bubble size was around 2 mm. A slight change in the transit time (velocity) observed with the presence of more nitrogen bubbles is probably due to the improved suspension. The theoretical

ultrasonic propagation of polystyrene spheres in water and glass spheres in epoxy systems has been studied by Anson and Chivers (28). Although their systems are not the same as in this study, their theoretical approaches - an effective medium approach, and a multiple scattering approach - can be applied to further theoretical study. The results from our study are in qualitative agreement with those previously reported by Okamura et al., (10). Our results with molten wax similar to the previous results from the nitrogen/water/glass beads system (26). However, our previous results for the nitrogen/water/glass beads system give larger values of time ratio at a given solids concentration fraction than our current nitrogen/paraffin wax/glass beads data. A possible explanation of this discrepancy could be that the geometry of our previous apparatus and nitrogen/water/glass bead system differs considerably from that employed here. In general, both the amplitude and the fractional change of transit time (or time ratio) were affected by the variation of solids concentrations. It appears that the time ratio depends mainly on the solids concentration. The variation of nitrogen flow has little effect on the observed fractional change of transit time (or time ratio) within the flow conditions studied.

We have noticed that the temperature of the paraffin wax has a significant effect on the ultrasonic signal. The effect of P-200 wax temperature on ultrasonic measurement under the conditions of a constant stirring speed and no gas flow in the autoclave reactor is plotted in Figure 12. It shows that the measured transit time and amplitude ratio become significantly influenced by the P-200 wax temperature. The increasing transit time and decreasing amplitude ratio as the temperature increased are probably due to the change in densities and other physical properties in the paraffin wax which result in the variation of the ultrasonic signal with temperatures. Based on these results, it can be concluded that the ultrasonic technique with some modifications has potential applications for solids concentration measurements in three-phase slurry reactors.

SUMMARY

Based on the three-phase experimental hydrodynamic studies, we can tentatively conclude that the addition of 20 wt% glass beads in the system has a slight effect on the average gas holdup and bubble size.

A well-posed three-dimensional hydrodynamic model was developed from a previous ill-posed model. The new model has shown reasonable solid holdup distributions in the column. The artificial "fountain" incorrectly predicted by the ill-posed model has been resolved. The program can be used for liquid-solids flows and with some modifications for gas-liquid-solids flows. The code is undergoing improvements such as extension to multisize particles, finite element, and parallelization to speed up running time.

The results presented in this study led to the conclusion that both the amplitude and the transit time of an ultrasonic signal are influenced by the variation of solids concentration in molten paraffin wax. The variation of nitrogen flow has little influence on the observed transit time within the conditions studied. The ultrasonic technique with some modifications has potential applications for solids concentration measurements in three-phase slurry reactors at elevated operating temperature.

ACKNOWLEDGEMENTS

The authors appreciate the help from R. R. Anderson and C. E. Taylor. I. K. Gamwo would like to acknowledge the support of the U.S. Department of Energy through ORISE.

NOMENCLATURE

D_{32}	Sauter mean diameter
C	Fluctuating velocity of particle
e	Coefficient of restitution
g	Gravity
g_0	Radial distribution function
[I]	Unit tensor
P	Pressure
q	Flux vector of fluctuating energy
t	Time
v	Velocity vector
a	Bubble or particle radius, m
A	Amplitude of the transmitted signal
A_o	Amplitude of the transmitted signal in the absence of nitrogen and solid
k	The wave number (k) of the ultrasonic wave which surrounds the bubble or particle
$f(d_b)$	A function dependent on the Sauter mean diameter
t_a	Arbitrary first distinct zero crossing time in liquid, s
t_b	Arbitrary first distinct zero crossing time in the presence of solid in slurry, s
t_o	Arbitrary travel time of the sound wave between the transmitter and the receiver in the absence of solid in slurry, s
v_l	Speed of sound in liquid, m/s
v_s	Speed of sound in solid, m/s
Δt	Equals $(t_a - t_b)$, s
$\Delta t/t_o$	Time ratio
x	The travel distance in the path, m
S( )	The scattering coefficient

Greek Letters

ν_l	Kinematic viscosity of liquid
ϵ_g	Gas holdup
σ_l	Surface tension
$ß_{km}$	Interphase momentum transfer between phase k and phase m
γ	Collision energy dissipation
ϵ	Volume fraction
$3/2\Theta_s$	Fluctuation energy
κ	Conductivity of fluctuating energy
μ	Shear viscosity
μ_s	Shear viscosity x volume fraction of solids
ξ_s	Bulk viscosity x volume fraction of solids
ξ	Bulk viscosity
ρ	Density
τ	Stress
α	A constant for particles at a given composition
ω	Solids concentration fraction
Γ	The volumetric interfacial area

Subscript

dil	Dilute

g Gas phase
k Phase k
l Liquid phase
m Phase m
s Solid phase

REFERENCES

1. S. C. Saxena, D. Patel, D. N. Smith, and J. A. Ruether, Chem. Eng. Comm., 63, 87 (1988).
2. Y. T. Shah, B. K. Kelkar, S.P. Godbole, and W. D. Deckwer, AIChE J., 28, 353 (1982).
3. D. B. Bukur, J. G. Daly, and S. A. Patel, AIChE J., 36, 93 (1990).
4. J. C. Kuo, DOE Final Report, DE-AC22-83PC60019 (1985).
5. E. S. Sanders, E. L. Ledakowicz, and W. D. Decker, Can. J. Chem. Eng., 64, 133 (1986).
6. W. D. Deckwer, Y. Loiisl, A. Zaldi, and M. Ralek, Ind. Eng. Chem. Process. Des. Dev., 19, 699 (1980).
7. R. W. Lyczkowski, D. Gidaspow, C. W. Solbrig and E. D. Hughes, Nucl. Sci. and Eng., 66, 378 (1978) .
8. I. K. Gamwo, Y. Soong, D. Gidaspow and R. W. Lyczkowski, Proc. 13th Int. Conf. on Fluidized Bed Combustion, Vol. 1, pp. 297-303, ASME, (1995).
9. J. X. Bouillard, R. W. Lyczkowski, and D. Gidaspow, AIChE J., 35, 6, 908, (1989).
10. S. Okamura, S. Uchida, T. Katsumata, and K. Iida, Chem. Eng. Sci., 44, 196 (1989).
11. Y. Soong, J. J. Boff, F. W. Harke, A. G. Blackwell, and M. F. Zarochak, Proc. Coal Liquef. and Gas to Liq. Contr. Rev. Conf., 897 (1994).
12. A. Matsura and L. S. Fan., AIChE J., 30, 894 (1984)
13. G. E. H. Joosten, J. G. H. Schilder, and J. J. Jansen, Chem. Eng. Sci. 32, 563 (1977).
14. Y. Kato, A. Nishiwaki, T. Fukuda, and S. Tanaka, J. Chem. Eng. Japan., 5, 112, (1972).
15. Y. M. Kato, and A. Nishiwaki, Int. Chem. Eng., 12, 182 (1972).
16. H. Hammer, Int. Chem. Eng. 21, 173 (1981).
17. J. Chabot., and H. I. de Lasa, AIChE Annual meeting, Nov 1-6, 1992, Miami, FL
18. D. B. Bukur, J. G. Daly, and S. A. Patel, DOE Report, DE-AC22-86PC90012, (1990).
19. G. Rudinger, and A. Chang, Physics of Fluids, 7, 1747 (1964).
20. G. A. Saltanov, 1972, Supersonic Two-Phase Flow, Moscow, USSR
21. R. W. Lyczkowski, AIChE Symp. Ser., 75 (174):165-174, (1978).
22. D. Kunii, and O. Levenspiel, 1969, Fluidization Engineering, Wiley, NY.
23. Gidaspow, D., and Ding, J., DOE Report, DOE-PC-89769, March 1990.
24. J. S. Chang., Y. Ichikawa, G. A. Irons., E. C. Morala.,and P. T. Wan, Measuring Techniques in Gas Liquid Two-Phase Flows, Delhaye, J.M. and Cognet, G., Eds, Springer-Verlag, 319 (1984).
25. H. P. Bensler., J. M. Delhaye., and C. Favreau., Proc. ANS National Heat Transfer Confer. 240 (1987).
26. Y. Soong., I. K. Gamwo, A. G. Blackwell, R. R. Schehl, and M. F. Zarochak, Chem. Eng. J. (1995) in press.
27. D. McClements, J. Adv. Colloid Int. Sci. 37, 33 (1991).
28. L. W. Anson., and R. C. Chivers., J. Acoust. Soc. Am. 85, 535 (1989).

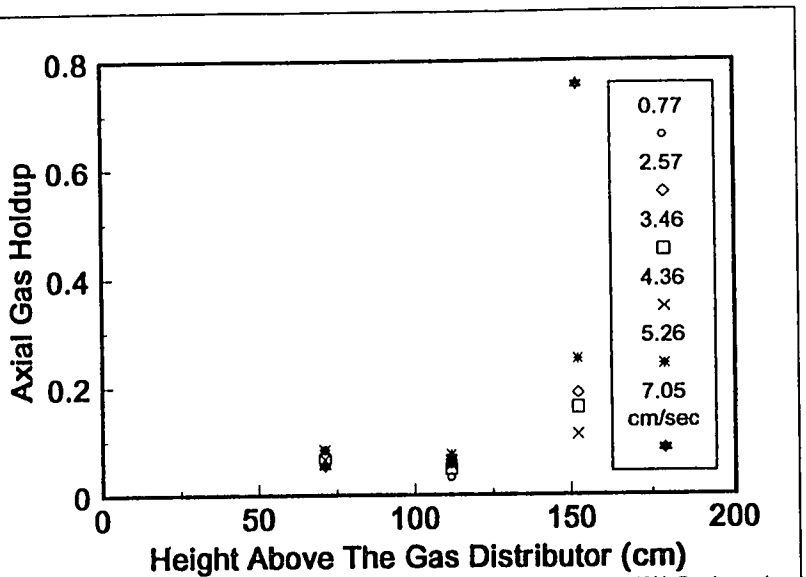

Figure 1. Effect of SFGV on Axial Gas Holdup in N2/Oil/Beads (20 wt%) System at Ambient Condition.

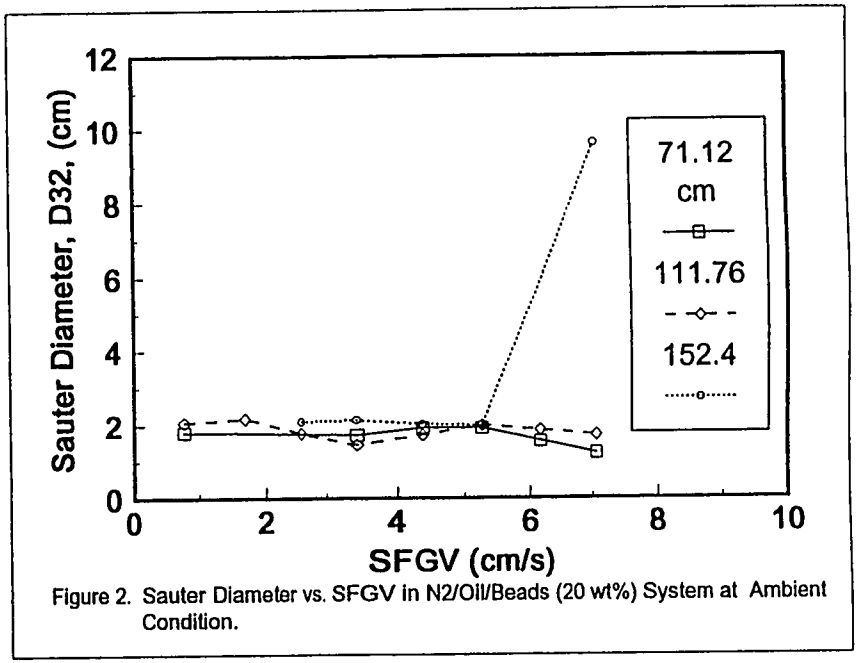

Figure 2. Sauter Diameter vs. SFGV in N2/Oil/Beads (20 wt%) System at Ambient Condition.

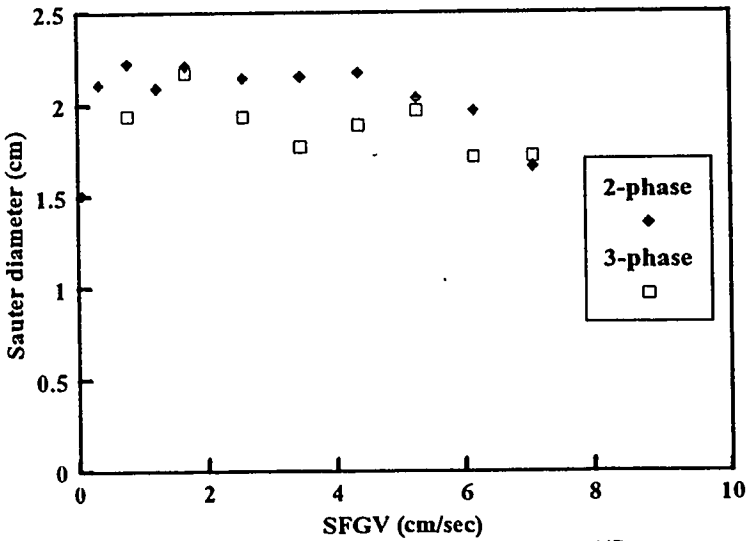

Figure 3 Effect of Solids and SFGV on Bubble Size at 20 °C and 0.1 MPa.

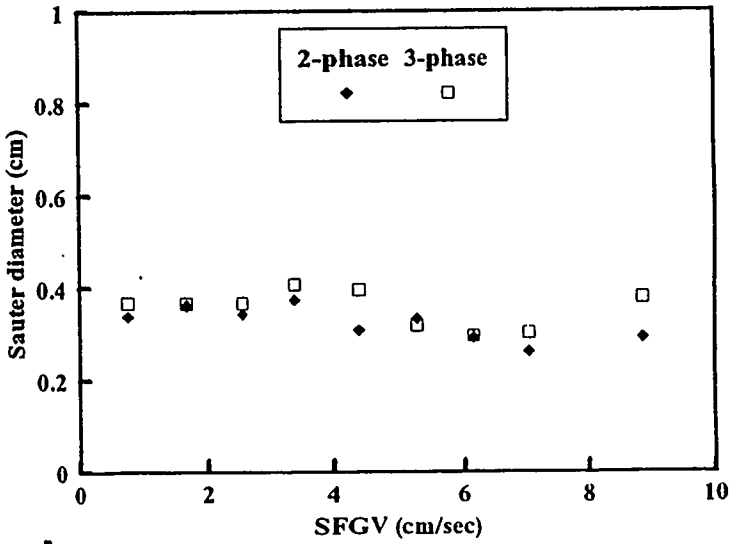

Figure 4. Effect of Solids and SFGV on Bubble Size at 200 °C and 1.36 MPa

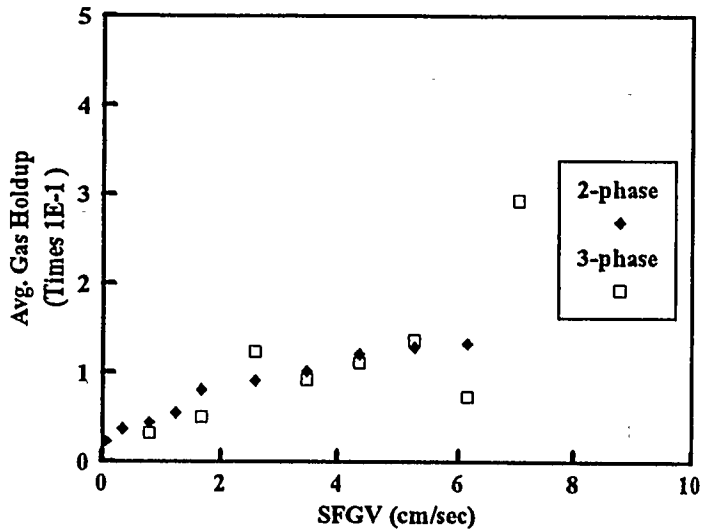

Figure 5. Effect of Solids (20wt%) and SFGV on Gas Holdup at 20°C and 0.1 MPa

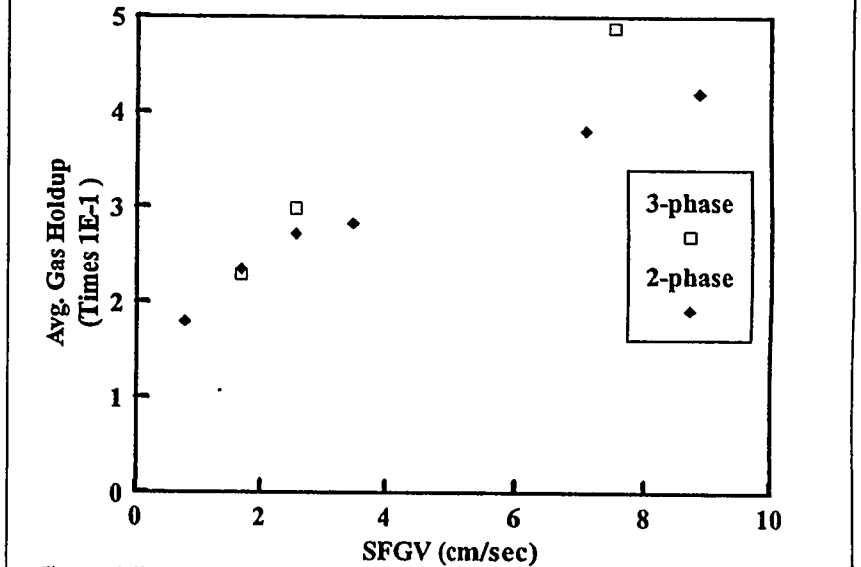

Figure 6. Effect of Solids (20wt%) and SFGV on Gas Holdup at 200°C and 1.36 MPa

DX min = 0.3175 cm
DY min = 0.3175 cm
DZ min = 2.1 cm

DX max = 3.0 cm
DY max = 0.635 cm
DZ max = 5.0 cm

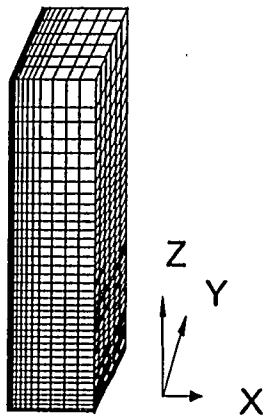

Figure 7. Finite Difference Cells.

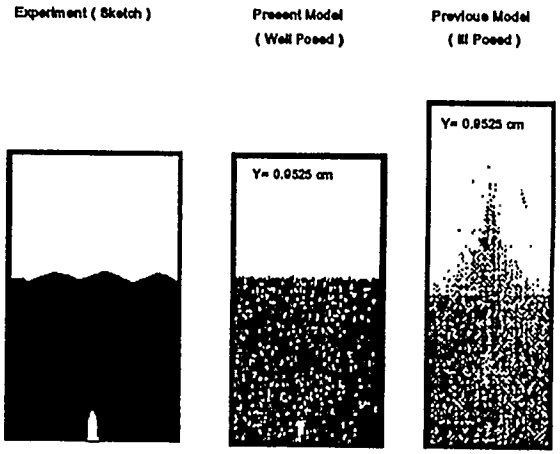

Figure 8. Comparison of Well-Posed and Ill-Posed Models Results with the Experiment (Sketch)

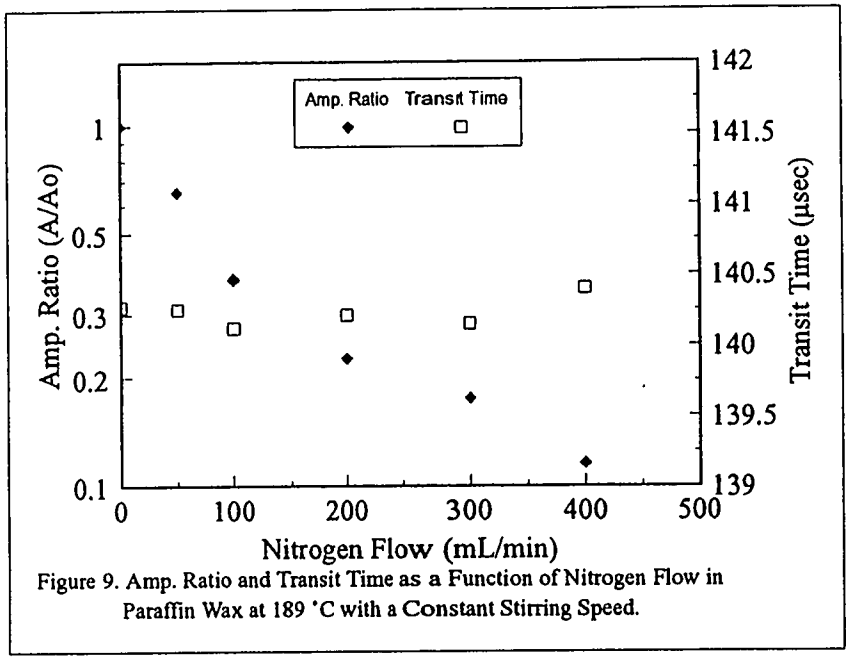

Figure 9. Amp. Ratio and Transit Time as a Function of Nitrogen Flow in Paraffin Wax at 189 °C with a Constant Stirring Speed.

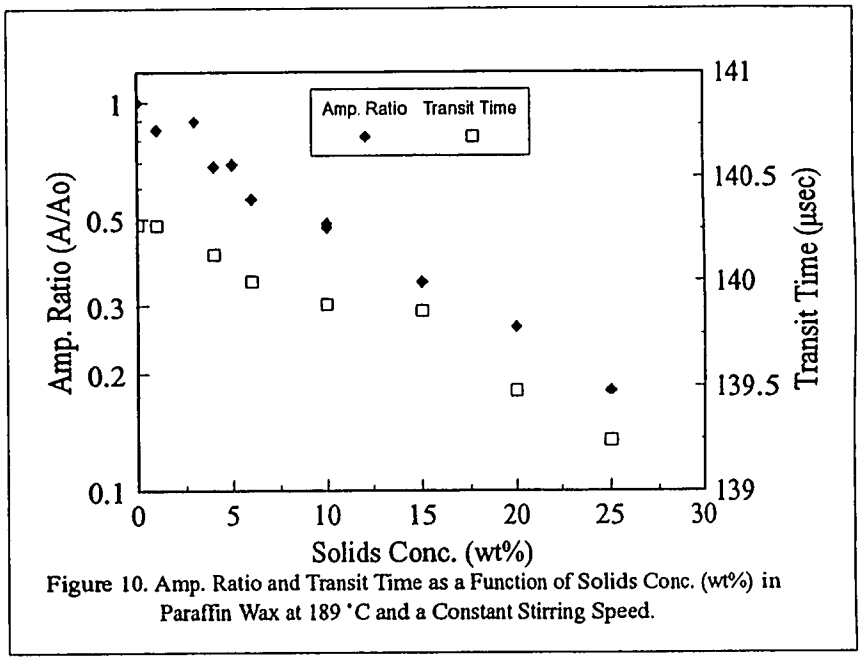

Figure 10. Amp. Ratio and Transit Time as a Function of Solids Conc. (wt%) in Paraffin Wax at 189 °C and a Constant Stirring Speed.

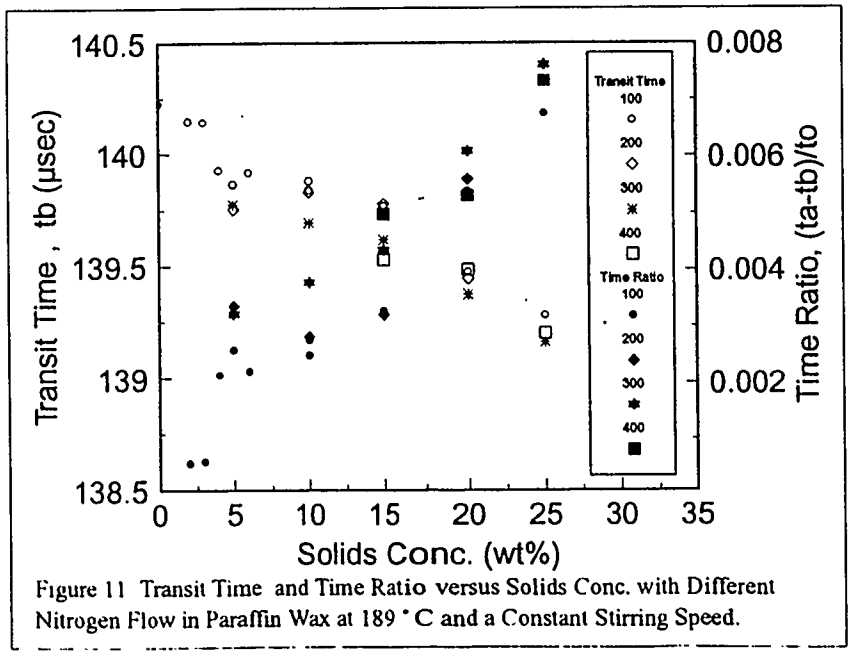

Figure 11 Transit Time and Time Ratio versus Solids Conc. with Different Nitrogen Flow in Paraffin Wax at 189 °C and a Constant Stirring Speed.

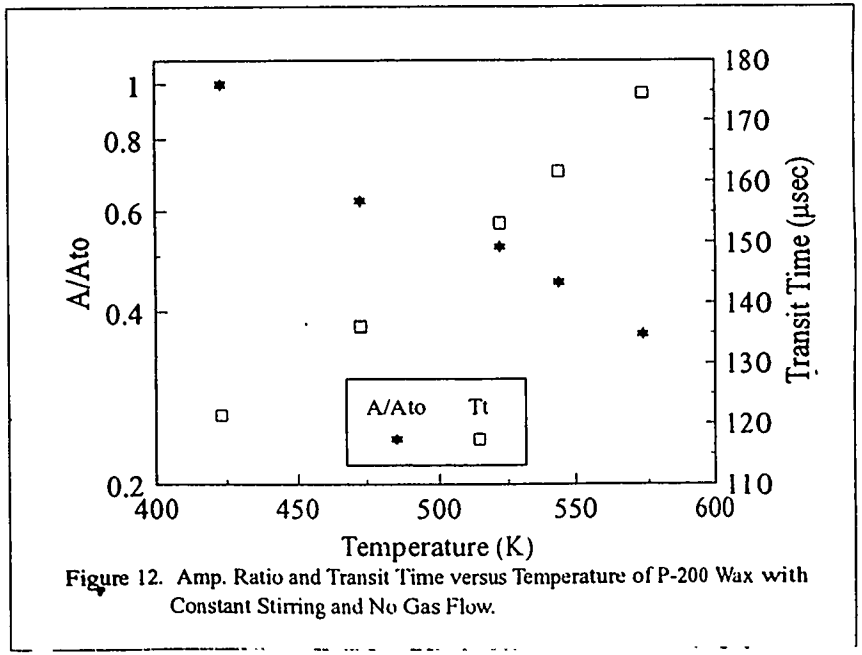

Figure 12. Amp. Ratio and Transit Time versus Temperature of P-200 Wax with Constant Stirring and No Gas Flow.